Surface acoustic waves on GaAs/$Al_xGa_{1-x}As$ heterostructures

A. Wixforth,* J. Scriba, M. Wassermeier, and J. P. Kotthaus
Institut für Angewandte Physik, Universität Hamburg, Jungiusstrasse 11, D-2000 Hamburg 36, West Germany

G. Weimann
Walter-Schottky-Institut, Technische Universität München, D-8046 Garching bei München, West Germany and Forschungsinstitut der Deutschen Bundespost, D-6100 Darmstadt, West Germany

W. Schlapp
Forschungsinstitut der Deutschen Bundespost, D-6100 Darmstadt, West Germany
(Received 6 March 1989)

The interaction between surface acoustic waves and quasi-two-dimensional inversion electron systems on GaAs/$Al_xGa_{1-x}As$ heterojunctions is investigated in high magnetic fields and at low temperatures. The interaction of the surface acoustic wave with high-mobility inversion electrons leads to strong quantum oscillations in both the transmitted surface wave intensity as well as in the sound velocity, reflecting the quantum oscillations of the magnetoconductivity as a function of an applied magnetic field. We study the dependence of this interaction on the magnetic field and on the surface-acoustic-wave power and frequency, and discuss the results using simple models. The influence of slight spatial inhomogeneities in the carrier density on the line shape of the quantum oscillations is analyzed in detail and related to their influence on the quantum Hall effect. First experimental results on the interaction of surface acoustic waves with two-dimensional electron systems in gated heterojunctions providing an adjustable carrier density are presented.

I. INTRODUCTION

Quasi-two-dimensional electron systems (2DES) as realized in space-charge layers on semiconductors have been studied extensively for about twenty years.[1] Various spectroscopic methods[1-3] as well as quasistatic methods such as dc conductance, magnetocapacitance,[4] or measurements of the electronic specific heat[5] have been used for investigations of the electronic properties of such a 2DES. The discovery of the integer quantum Hall effect[6] (QHE) as well as the fractional quantized Hall effect[7] (FQHE) led to a strong interest in the properties of the 2DES in very-high-mobility samples in high magnetic fields and at low temperatures.

Also the interaction between electrons in a 2DES and acoustic phonons has attracted much attention.[8] Direct studies of phonon absorption[9] and emission[10] by a 2DES have been carried out with ballistic phonons at THz frequencies. Here, we wish to review recent investigations of the magnetically quantized 2DES using surface acoustic waves (SAW) in the radio frequency regime.[11,12] Corresponding to the comparably low sound velocity, the wavelengths λ of these lattice vibrations are in the 10 μm range. We show that on piezoelectric semiconductors such as GaAs the interaction between the SAW's and the 2DES in this wavelength range is dominated by the piezoelectric field accompanying the SAW's. Thus our experiments may be regarded as intermediate between spectroscopic investigations of the 2DES using microwave radiation[13] and quasistatic transport experiments. As it turns out, electron SAW interaction is very sensitive in the regime of very small conductivities σ. Hence our experiments are very well suited to study the 2DES in situations where its conductivity is very small. This is the case at high magnetic fields in the QHE regime near integer filling factors ν of Landau levels or at $B=0$ near inversion threshold. On semiconductors, surface waves have previously been used to study surface properties[14] taking advantage of the fact that the SAW is concentrated only within a relatively thin layer at the sample surface.

In Sec. II of this report, we first give a short review of some main aspects and features of surface acoustic waves[15] on piezoelectric semiconductors like GaAs. Then we will model the 2DES as a very thin conducting layer on the surface of a piezoelectric insulator. In Sec. III we briefly describe the samples used and the experimental techniques involved in our experiments. We will discuss two different experimental techniques, one, in which the SAW propagates directly on the semiconductor under investigation and another where the SAW propagates on a strongly piezoelectric insulator in close proximity to the sample studied.[16,17] In the latter case, a sandwich-type configuration is used, consisting of a $LiNbO_3$ delay line and the GaAs sample under investigation. In Sec. IV we present and discuss our experimental results. We first describe the influence of a magnetically quantized 2DES on the transmitted SAW intensity and sound velocity. We then quantitatively explain the observed quantum oscillations using a relaxation-type model outlined in Sec. II. The next section focuses on the power dependence of the interaction between a SAW and

a 2DES. Here, we demonstrate that the 2DES can be heated by the electric field of the SAW. Then we concentrate on the line-shape analysis of the observed quantum oscillations and point out the importance of small spatial inhomogeneities in the carrier density.[18] This section is followed by a brief discussion of the observed frequency dependence of the interaction of a SAW and a 2DES. Finally, we present initial observations of this interaction in gated heterojunctions. Here the carrier density in the 2DES can be controlled by a front gate electrode via field effect.

II. SURFACE WAVES ON PIEZOELECTRIC HETEROSTRUCTURES

Surface acoustic waves are modes of elastic energy propagating along the surface of an elastic medium. The displacement amplitudes essentially decay in an exponential fashion into the bulk. Hence, the main energy flow is concentrated within a distance of the order of a wavelength λ beneath the surface. The particle displacement at and beneath the surface is elliptic, leading to an elliptical polarization of the wave.

Here we shall focus on the case where a SAW is propagating on a semi-insulating piezoelectric semiconductor such as GaAs, having near its surface a quasi-two-dimensional electron system. We limit our discussion to crystal cuts and propagation directions which are piezoelectrically active, i.e., where the SAW is accompanied by an electric field. We will show that this piezoelectrically induced field is the dominant cause for the interaction between a SAW and a 2DES in heterostructures.

The basic equations of state that govern the propagation of elastic waves in a piezoelectric material connect the mechanical stress T and the electrical displacement D with the mechanical strain S and the electric field E.[15] In a simplified one-dimensional form these are

$$T=cS-eE \quad \text{and} \quad D=eS+\epsilon E \ . \tag{1}$$

Here c is the stiffness constant, e the piezoelectric constant, and ϵ the electric permittivity of the crystal under consideration. The above "elastic" equation is Hooke's law extended by the additional stress $-eE$ due to the piezoelectric effect. The "electrical" equation for D includes the electrical polarization eS produced by the strain S. Generally the above equations have to be written in tensor form, taking into account the anisotropy and the symmetry of the crystal and, for a SAW, its surface. For simplicity, we restrict our discussion to the one-dimensional model directly applicable only for longitudinal bulk waves. Using

$$\frac{\partial S}{\partial x}=\frac{\partial^2 u}{\partial x^2} \quad \text{and} \quad \frac{\partial T}{\partial x}=\rho\frac{\partial^2 u}{\partial t^2} \tag{2}$$

where u is the displacement amplitude in the x direction and ρ the density of the material, one obtains a wave equation for the problem, namely,

$$\rho\frac{\partial^2 u}{\partial t^2}=c\left[1+\frac{e^2}{c\epsilon}\right]\frac{\partial^2 u}{\partial x^2}-\frac{e}{\epsilon}\frac{\partial D}{\partial x} \ . \tag{3}$$

Using this wave equation for homogeneous bulk materials we now can discuss two limiting cases: If the material is a very good piezoelectric conductor, with conductivity $\sigma\simeq\infty$, the internal electric field has to vanish. Equation (3) thus describes longitudinal sound waves in a medium which appears to be nonpiezoelectric. The sound velocity then is $v_0=\sqrt{c/\rho}$. If, on the other hand, the material is a piezoelectric insulator, i.e., $\sigma=0$, Poisson's equation requires $\partial D/\partial x=0$. Then, Eq. (3) describes plane waves in a medium with increased elastic constants $c'=c(1+e^2/c\epsilon)$ and thus $v=\sqrt{c'/\rho}$. This effect is called piezoelectric stiffening and is used to define the electromechanical coupling coefficient K^2 as a measure of strength of the piezoelectricity of a given material. Since $e^2/c\epsilon$ usually is a small quantity, it is convenient to define the piezoelectric coupling coefficient

$$K^2=\frac{e^2}{c\epsilon}\simeq\frac{2(v-v_0)}{v_0} \ . \tag{4}$$

Usually K^2 is less than 0.05 for all piezoelectric materials. For surface waves, one obtains an effective coupling coefficient K_{eff} that differs slightly from the one derived in Eq. (4) using bulk elastic constants since boundary conditions at the crystal surface have to be taken into account. For a (100) surface on GaAs, with a SAW propagating in the piezoelectric [011] direction, one finds $K^2_{\text{eff}}=6.4\times10^{-4}$.[19]

The propagation of a SAW on a piezoelectric semiconductor with homogeneous bulk conductivity σ has been analyzed by several authors[20,21] and we restrict ourselves here to summarizing the essential results. The longitudinal electric field E accompanying the SAW propagating with the characteristic sound velocity can couple to the mobile carriers in the material. This leads to induced currents and results in Ohmic loss σE^2. Since power is transferred from the SAW, the wave will be attenuated. Simultaneously, the sound velocity is altered by the piezoelectric stiffening of the material. The attenuation and the change in SAW velocity as a function of the conductivity σ in the case of a homogeneous piezoelectric conductor are, respectively,[20]

$$\Gamma=\frac{\omega}{v_0}\frac{K^2_{\text{eff}}}{2}\frac{(\omega_c/\omega)}{1+(\omega_c/\omega)^2} \tag{5}$$

and

$$\frac{\Delta v}{v_0}=\frac{K^2_{\text{eff}}}{2}\frac{1}{1+(\omega_c/\omega)^2} \ . \tag{6}$$

Here, $\omega_c=\sigma/(\epsilon_1+\epsilon_2)$ is the conductivity relaxation frequency, ϵ_1 and ϵ_2 are the dielectric constants of the piezoelectric substrate and the half-space above it, respectively.[21] This conductivity relaxation frequency is the inverse of the time constant in which the electron system relaxes from a perturbation by an external electric field into its equilibrium distribution. If the ultrasonic frequency ω is much lower than ω_c, the carriers will be able to redistribute rapidly enough to screen the external piezoelectric field. If the frequency ω is comparable or larger than ω_c this screening becomes less perfect and

finally at $\omega \gg \omega_c$ the piezoelectric field will be nearly the same as for a corresponding insulator. Maximum attenuation occurs at $\omega = \omega_c$ and piezoelectric stiffening is observed only for $\omega \gtrsim \omega_c$.

We now consider the case of a 2DES which we simply model by a thin sheet of mobile carriers with sheet conductivity $\sigma_\square$ located directly on top of the crystal. The thickness d of this conducting layer is assumed to be much smaller than the wavelength of the SAW. Then the longitudinal electric field of the SAW can only be screened at the surface, i.e., $z = 0$. This effect is illustrated in Fig. 1 where the normalized SAW electric potential as a function of depth in the material for both cases $\sigma_\square = 0$ and $\sigma_\square = \infty$ is shown. One clearly sees how the SAW potential recovers with distance from the conducting surface. Equations (5) and (6) used above for the homogeneous semiconductor apply here, too. The fact that here the conductivity is restricted to a thin sheet results effectively in a modification of the relaxation frequency ω_c. As shown by several authors[22–25] this relaxation frequency ω_c now becomes dependent on the wave vector of the SAW $k = 2\pi/\lambda$. Now, only a thin conducting sheet of thickness $d \ll \lambda$ and sheet conductivity $\sigma_\square = \sigma d$ carries the induced currents. This is reflected in an increase of the effective resistance by a factor $1/kd$.[22] Hence, the conductivity relaxation frequency now becomes

$$\omega_c = \frac{\sigma_\square k}{\epsilon_1 + \epsilon_2} . \tag{7}$$

Thus, for the 2D case, the ratio ω_c/ω in Eqs. (5) and (6) has to be replaced by the frequency-independent ratio $\sigma_\square/\sigma_M$ where $\sigma_M = v_0(\epsilon_1 + \epsilon_2)$ and we have

$$\Gamma = k \frac{K_{\text{eff}}^2}{2} \frac{\sigma_\square/\sigma_M}{1 + (\sigma_\square/\sigma_M)^2} , \tag{8}$$

$$\frac{\Delta v}{v_0} = \frac{K_{\text{eff}}^2}{2} \frac{1}{1 + (\sigma_\square/\sigma_M)^2} . \tag{9}$$

This is true for frequencies $\omega \ll 1/\tau_t$ where τ_t is the transport relaxation time of the 2DES. For these frequencies $\sigma_\square$ can be regarded as frequency independent. Also, Eqs. (8) and (9) are restricted to the local regime, i.e., $d \ll \lambda$ and $l_{\text{int}} \ll \lambda$ where l_{int} is an intrinsic length in the 2DES such as the electronic mean free path. Figure 2 illustrates Eqs. (8) and (9), i.e., the attenuation Γ per unit length as well as the relative change $\Delta v/v_0 = (v - v_0)/v_0$ of the sound velocity as a function of the sheet conductivity $\sigma_\square$ of a 2D layer. For the special case of a (100) GaAs surface with $\mathbf{k}_{\text{SAW}} \| [011]$ the characteristic conductivity σ_M is about $3.3 \times 10^{-7} \Omega_\square^{-1}$.

For conductivities $\sigma_\square \ll \sigma_M$ the attenuation per unit length is proportional to the conductivity, for $\sigma_\square \gg \sigma_M$ it is proportional to $1/\sigma_\square$. The sound velocity changes in a rather steplike fashion in the vicinity of $\sigma_\square = \sigma_M$ between the two limiting cases discussed above.

Since our experiments are mostly carried out in magnetic fields applied perpendicularly to the heterojunction, we have to consider the magnetic-field-induced anisotro-

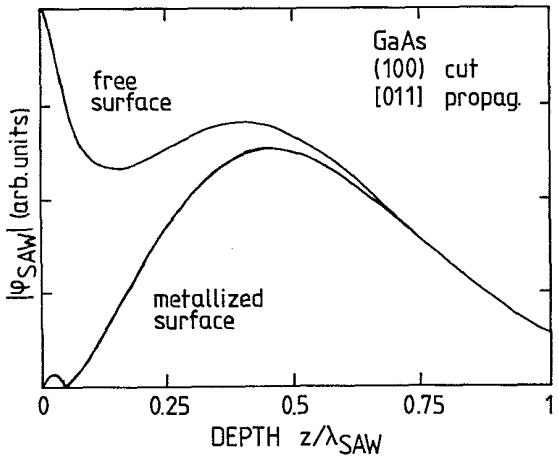

FIG. 1. Absolute value of the SAW electric potential $|\phi_{\text{SAW}}|$ as function of depth into bulk in units of the SAW wavelength λ. Both cases of free ($\sigma_\square = 0$) and metallized ($\sigma_\square = \infty$) GaAs surface are depicted (after Ref. 37).

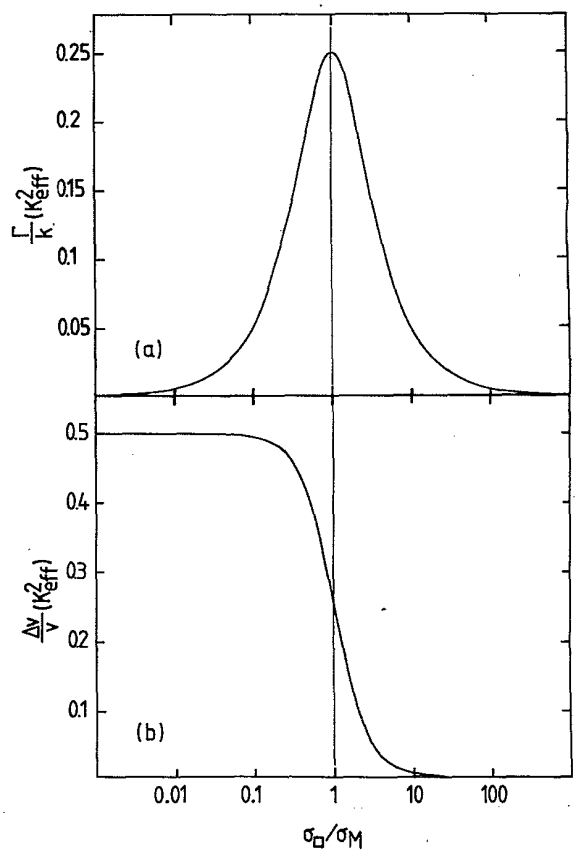

FIG. 2. Attenuation coefficient Γ per unit wave vector k (a) and change in sound velocity $\Delta v/v_0$ (b) in units of K_{eff}^2 as a function of the sheet conductivity $\sigma_\square$ of the 2DES which is assumed to be located on top of the crystal surface. The conductivity $\sigma_\square$ is given in units of σ_M as defined in the text.

py of the conductivity, expressed by the magnetoconductivity tensor. If the longitudinal electric field in the SAW defines the x direction, the sheet conductivity $\sigma_\square$ in Eqs. (8) and (9) has to be replaced by the diagonal tensor component σ_{xx}. We want to emphasize that here the interaction between a surface acoustic wave on a piezoelectric substrate and a 2DES is only described by the interaction of the longitudinal electric field of the SAW with the mobile carriers. This piezoelectric interaction can be described completely classically and is of relaxation type. The deformation potential interaction turns out to be negligible in comparison to the piezoelectric interaction for frequencies up to several GHz.[26] Thus we omit it in the discussion of our experiments.

III. EXPERIMENTAL NOTES

For our experiments we use two configurations with the SAW either propagating on the heterostructure itself or on a piezoelectric insulator brought in close contact to the heterostructure of interest, as discussed in the following. In a later section we will consider the experimental requirements necessary to study gated heterojunctions with SAW's.

A. Direct coupling

A sketch of a typical sample configuration used to study the interaction of a SAW propagating on the semiconductor structure containing the 2DES is shown in Fig. 3. We start with conventional GaAs/$Al_xGa_{1-x}As$ heterojunctions grown by molecular-beam epitaxy[27] (MBE) on a semi-insulating (100) GaAs substrate. A part of the MBE-grown layer containing the high-mobility 2DES is chemically removed to define a conventional Hall bar mesa. Indium diffused contacts allow us to simultaneously measure ρ_{xx} and ρ_{xy} of the 2DES in a magnetic field. On both sides of this mesa we fabricate interdigital transducers[28] forming a SAW delay line. They are prepared directly on the semi-insulating GaAs substrate to avoid capacitive coupling to the 2DES. The crystal cut used here (i.e., (100) surface, [110] propagation) results in the highest achievable electromechanical coupling coefficient for surface waves on GaAs.

In the heterojunction, the thickness of the GaAs cap layer, the Si-doped $Al_xGa_{1-x}As$ layer, and the undoped spacer add up to typically 100 nm and thus are much smaller than the SAW penetration depth. Our experiments are carried out at low temperatures ($T \lesssim 4.2$ K) and in high magnetic fields ($B \lesssim 12$ T) applied perpendicularly to the surface of the sample. The SAW delay line operates at a fundamental wavelength $\lambda = p$, where p is the period of the interdigital transducer structure. As sketched in Fig. 4 a radio frequency $f_0 = v/p$ is fed into one of the transducers to generate a coherent and monochromatic SAW. With short rf pulses (0.1–1 μsec) we periodically produce SAW packets at typical repetition rates of 10 kHz that are transmitted through the heterojunction and detected after typical delay times of 2 μsec at the opposite transducer. Then they are amplified and analyzed in phase and intensity using the experimental setup as depicted in Fig. 4. The SAW intensity is recorded with a diode detector. The phase deviation due to the interaction with the 2DES is obtained by homodyne mixing using a phase-locked loop (PLL) that keeps the phase difference between signal and reference constant by controlling the generator frequency. This frequency change is recorded and calibrated in units of velocity change, using $\Delta v/v = (\Delta f/f) l/L$. Here l is the spatial separation of the two transducers on the sample and L is the length of the interaction region, i.e., the length of the Hall bar containing the 2DES. Standard boxcar integrating techniques then provide signals proportional to the SAW intensity and phase, respectively, as a function of the magnetic field B. A typical SAW intensity signal as measured at the boxcar input is displayed in Fig. 5. By special design of the transducers the excitation of higher harmonics of the fundamental frequency f_0 is also possible. This is illustrated in Fig. 6, where the frequency spectrum of a typical SAW delay line on GaAs is depicted.

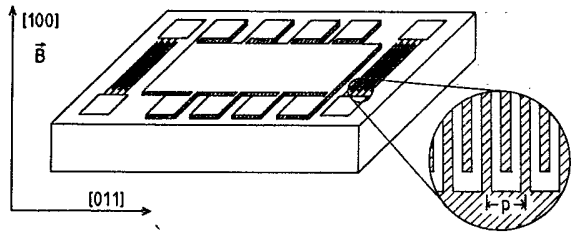

FIG. 3. Typical sample geometry as used in SAW experiments. On standard MBE-grown heterostructures we prepare a Hall bar-shaped active mesa containing the high-mobility 2DES. Interdigital transducers are fabricated photolithographically directly onto the GaAs substrate. The inset shows a section of a transducer. The SAW wavelength λ is given by the periodicity p of the transducer (from Ref. 11).

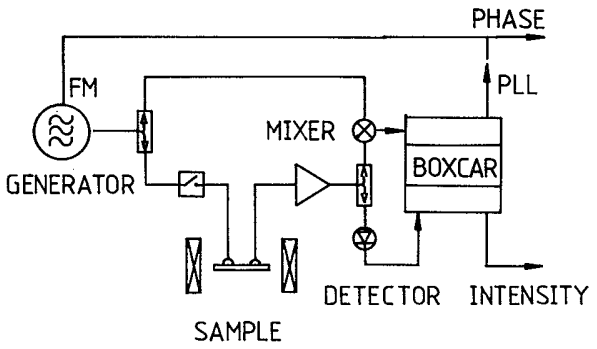

FIG. 4. Schematic diagram of the experimental setup used to investigate the interaction between a SAW and a 2DES as explained in the text. The sample is located in the center of a superconducting solenoid at low temperatures.

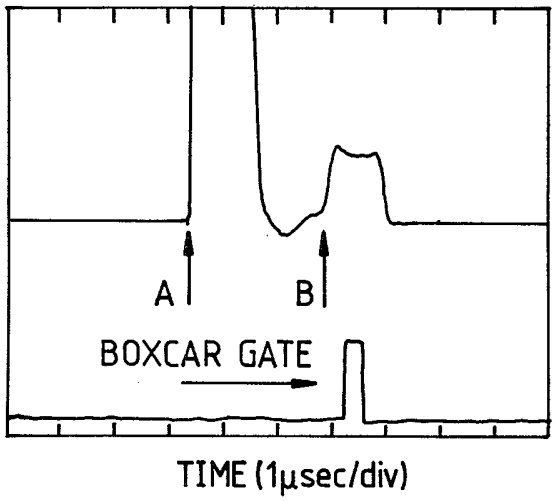

FIG. 5. Typical oscilloscope trace of the received SAW intensity signal as measured with the diode detector. At time A the emitting transducer launches a short SAW packet (0.2–1 μsec) which reaches the receiver at time B. The signals at B can be separated from the electromagnetic pickup by use of standard boxcar integrating techniques.

B. Proximity coupling

Proximity coupling is another useful technique to observe the magnetoacoustic interaction between a SAW and a 2DES.[16,17] In this case the SAW is excited not on the heterostructure sample itself but on a separate piezoelectric substrate which is brought into intimate contact with the heterostructure. For this purpose we use Y-cut, Z-propagating $LiNbO_3$ delay lines, which have a very high electromechanical coupling coefficient ($K^2_{\text{eff}}=0.048$). Such an arrangement is shown in Fig. 7. The heterostructure sample is mechanically pressed face down on top of the delay line. If the air gap between the delay line and the heterostructure sample is considerably smaller than the wavelength of the SAW, the SAW electric field can penetrate into the sample and interact with the 2DES. This system is acoustically mismatched, so that the SAW propagates on the $LiNbO_3$ substrate only. For such a sandwich arrangement the characteristic conductivity σ_M in Eqs. (8) and (9) has to be replaced by a modified σ'_M depending also on kz_0, where z_0 is the thickness of the air gap.[16] The interaction between the SAW electric field of the delay line and the 2D electrons of the sample vanishes exponentially with the distance between the two components. Nonetheless, with a reasonable air gap z_0 of a few μm and SAW wavelengths of some 10 μm, the observed quantum oscillations in the amplitude and phase of the SAW signal are of the same order as those measured directly on GaAs. This is due to the fact that the coupling coefficient K_{eff} entering Eqs. (8) and (9) is now that of $LiNbO_3$ being bigger than that of GaAs by 2 orders of magnitude.

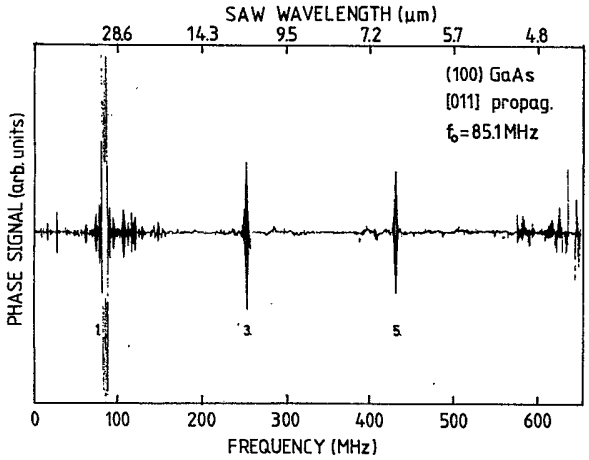

FIG. 6. Transmitted frequency spectrum of a SAW delay line having transducers with period $p=33$ μm as used in our experiments. Higher harmonics of the fundamental frequency f_0 can also be generated.

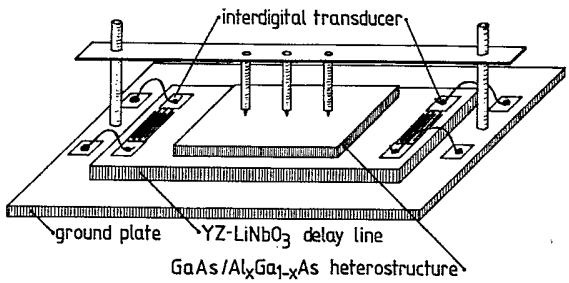

FIG. 7. Sketch of a sandwich system consisting of a Y-cut, Z-propagating $LiNbO_3$ SAW delay line and a $GaAs/Al_xGa_{1-x}As$ heterostructure. The sample is pressed face down onto the piezoelectric substrate on which the SAW propagates. Interaction with the 2DES is mediated via the SAW electric field, which penetrates into the heterostructure sample (from Ref. 17).

C. Gated heterostructures

We also study the interaction of a SAW and a 2DES in gated heterostructure samples. By the use of a front gate electrode and a gate voltage between this gate and the 2DES one is able to deplete the 2D channel of mobile carriers. The use of a front gate, however, directly affects the effectivity of the SAW technique. As shown in Sec. II, a metallized surface shortens the electric field of the SAW, and thus suppresses the interaction with the 2DES close to the surface. One can avoid such detrimental effects by either using back gates or gating across a thinned $LiNbO_3$ delay line. The latter techniques, however, usually limit the tunability of the carrier density in the 2DES and often cause problems with respect to homogeneity of the depleted 2DES. Hence we choose a gating technique where the front gate is kept at a certain distance from the 2DES. A suitable spacer is an insulating photoresist film of thickness $d=100-500$ nm with the gate electrode on top of it. Here, the surface wave propagates at the interface between insulator and sample

surface. Since the gate plane then is above the GaAs-resist interface, we expect the SAW field at the plane of the 2DES to be screened much less than it would be by a gate on the GaAs surface itself (see Fig. 1). Initial experimental results using gated heterostructure samples are given in Sec. IV E.

IV. EXPERIMENTAL RESULTS AND DISCUSSION

A. Quantum oscillations in the SAW propagation

As shown in Sec. II, SAW's are most sensitive to a conducting surface layer at relatively low sheet conductivities $\sigma_\square \simeq \sigma_M$. Therefore SAW experiments are appropriate to study regimes of low dynamic conductivity σ_{xx} of a 2DES that occur at low temperatures in quantizing magnetic fields B or, at $B=0$ T, near inversion threshold. In high magnetic fields the magnetoconductivity σ_{xx} of a high-mobility sample exhibits strong Shubnikov–de Haas oscillation, caused by the complete quantization of the energy spectrum of the 2DES. Deep minima of σ_{xx} are observed whenever the Landau level filling factor $\nu = N_s h/eB$, where N_s is the areal electron density in the 2DES, is close to an integer i ($i=1,2,3,\ldots$). Simultaneously the Hall resistance ρ_{xy} becomes quantized, i.e., $\rho_{xy} = h/(e^2 i)$. Thus SAW studies give a direct insight into the conductivity oscillations in the quantum Hall regime and might lead to a better understanding of the QHE.

Here, we want to discuss the influence of a completely quantized 2DES in a strong magnetic field on the propagation parameters of a SAW, transmitted through the heterojunction. The measured magnetic field dependencies of these parameters in a typical heterojunction, i.e., the transmitted SAW intensity and the change in SAW velocity $\Delta v/v_0$, are shown in Figs. 8(a) and 8(b), respectively. The measurements are made at sufficiently low SAW amplitudes to avoid nonlinear effects discussed in the following section. For comparison, Fig. 8(c) displays the magnetoconductivity $\sigma_{xx}(B)$ of the sample as deduced from measurements of $\rho_{xx}(B)$ and $\rho_{xy}(B)$ in Hall bar geometry.

At low magnetic fields ($B \lesssim 1$ T) the magnetoconductivity $\sigma_{xx}(B)$ changes by an order of magnitude due to the high mobility of the 2DES ($\mu \simeq 500\,000$ cm^2/V sec) in this sample. Therefore this region is omitted for clarity in Fig. 8(c). The SAW intensity [Fig. 8(a)] and the change in SAW velocity [Fig. 8(b)], however, remain nearly unchanged in this magnetic field range. At higher magnetic fields strong quantum oscillations appear in the SAW intensity $I(B)$ and in $\Delta v(B)/v_0$, which coincide in position with deep minima in $\sigma_{xx}(B)$. Deep minima in $\sigma_{xx}(B)$ always occur if the Fermi level is located between two Landau levels, i.e., for integer filling factors ν.

The quantum oscillations in the SAW intensity $I(B)$ appear different from those in $\sigma_{xx}(B)$ since the SAW attenuation [Eq. (8)] is not a linear function of $\sigma_{xx}(B)$. For the regime, where $\sigma_{xx}(B) < \sigma_M$, i.e., for high magnetic fields or low filling factors ν, the quantum oscillations in the SAW intensity reveal a characteristic feature. They are split into two distinct minima, which are neither observed in $\Delta v(B)/v_0$ nor in $\sigma_{xx}(B)$. This splitting is a kind of fingerprint of the interaction between a SAW and a 2DES in a strongly quantizing magnetic field. It occurs when $\sigma_{xx}(B)$ drops to very low values below σ_M. Traversing such a deep minimum, $\sigma_{xx}(B)$ passes σ_M twice, leading to the occurrence of two maxima in the attenuation $\Gamma(B)$ or, in turn, of two minima in the transmitted SAW intensity $I(B) = I_0 \exp(-\Gamma L)$. Here L is the length of the interaction region, i.e., the length of the Hall bar in propagation direction. The center maximum of $I(B)$ of such a split quantum oscillation then corresponds to the minimum values of $\sigma_{xx}(B)$.

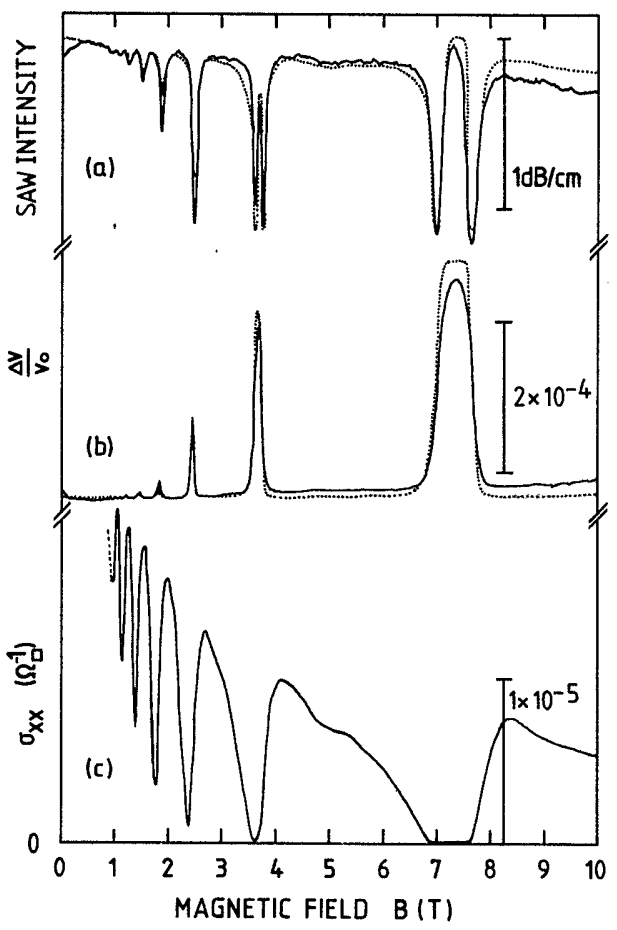

FIG. 8. SAW intensity $I(B)$ (a) and change in sound velocity $\Delta v/v_0$ (b) after transmission through a heterojunction with electron density $N_s = 3.5\times10^{11}$ cm^{-2} as function of the magnetic field B at a SAW wavelength $\lambda = 33$ μm and temperature $T = 4.2$ K. Trace (c) shows, for comparison, the magnetoconductivity $\sigma_{xx}(B)$ as extracted from measurements of $\rho_{xx}(B)$ and $\rho_{xy}(B)$ in Hall bar geometry. As explained in the text the quantum oscillations in $I(B)$ and in $\Delta v(B)/v_0$ reflect the oscillations of $\sigma_{xx}(B)$ in the regime of very low conductivities $\sigma_{xx} \simeq \sigma_M$. The dotted lines in (a) and (b) are the results of calculations using Eqs. (8) and (9) and σ_{xx} from (c). Best agreement between experiment and calculation is obtained by using $K^2_{\text{eff}} = 6.4\times10^{-4}$ and $\sigma_M = 4\times10^{-7}\Omega_\square^{-1}$ (from Ref. 11).

The effect of piezoelectric stiffening caused by the reduced screening of the SAW is clearly observed in Fig. 8(b). For each minimum in $\sigma_{xx}(B)$ the sound velocity increases, as predicted by Eq. (9). The dotted lines in Figs. 8(a) and 8(b) are the corresponding quantities calculated using Eqs. (8) and (9) and $\sigma_{xx}(B)$ from Fig. 8(c). To achieve best agreement between the calculation and the experimental data, we here used $\sigma_M = 4\times10^{-7}\Omega_\square^{-1}$ and $K^2_{\text{eff}} = 6.4\times10^{-4}$. This σ_M compares well with the one calculated above from the measured sound velocity and known dielectric constant ($\sigma_M = 3.3\times10^{-7}\Omega_\square^{-1}$), whereas the value used here for K^2_{eff} is the same as measured by other authors.[19] Figure 8 displays representative results for a given temperature and SAW wavelength. For lower temperatures and for higher SAW frequencies the agreement between our model and the experimental results is similarly satisfying. Nevertheless, for most samples we find small deviations from the predictions of the simple relaxation-type model discussed above. The most apparent difference is that the double minima in $I(B)$ do not have equal amplitudes as predicted by Eq. (8). We will discuss this phenomenon in Sec. IV C. Apart from these deviations, the classical conductivity relaxation model, as presented in Sec. II, provides a good description of the influence of a quantized 2DES in a strong magnetic field under QHE conditions on the SAW propagation parameters.

B. Power dependence

As demonstrated above, the interaction between a SAW and a 2DES is strongest in the regime of the QHE. In this regime, we also have studied the dependence of the SAW attenuation on incident power, i.e., on the amplitude of the SAW. A representative result of such investigations is given in Fig. 9 for four different power levels. Here the dependence of a given split quantum oscillation in the SAW intensity $I(B)$ around $\nu=4$ on incident SAW power is depicted. With increasing power the splitting of the oscillation disappears. One observes a decrease of the center maximum in $I(B)$ and simultaneously a decrease of the separation of the double minima on the B scale. At the highest power level in Fig. 9 both minima merge. The same behavior is observed for all split oscillations that occur at low temperatures. Oscillations corresponding to higher filling factors or equivalently to lower magnetic fields, however, begin to disappear at lower power levels.

Generally we use short SAW packets ($\simeq 1$ μsec) and sufficiently low repetition rates ($\simeq 10$ kHz) to avoid thermal heating of the whole sample. We interpret the observed power dependence as resulting from heating of the 2DES by the electric field of the SAW. The center maximum of a split oscillation in $I(B)$ corresponds to a deep minimum in $\sigma_{xx}(B)$ at integer filling factor ν. The Fermi level in this case lies in the center of the mobility gap between two adjacent Landau levels. An increasing electron temperature T_e thermally activates carriers from the lower Landau level to the higher one. Such an activation causes an increase of the minimum in $\sigma_{xx}(B)$, which in turn will lead to a decrease of the center maximum in $I(B)$. Electron heating by means of the SAW electric field is distinctly different from heating via a drift electric field applied between source and drain contacts. Since the SAW electric field is partially screened by the 2DES the field amplitude, for a given mechanical amplitude of the SAW, decreases with increasing conductivity of the electron gas as $E(\sigma_\square) = E_0(1+(\sigma_\square/\sigma_M)^2)^{-1/2}$. This has to be included in a quantitative analysis. Though we have performed such an analysis which can describe the experimental observations it presently contains too many unknown parameters to gain more physical insight. However, SAW traces measured at different lattice temperatures and low power levels show that heating of order 10 K is necessary to produce traces comparable to the highest power levels (Fig. 9).

To experimentally confirm that the thermal activation of $\sigma_{\min}$ is not induced by lattice heating but caused by electron heating of the free carriers alone and thus is quasi-instantaneous, we have fabricated a special sample with two pairs of transducers operating at different frequencies. One of them is fed with high-power rf bursts and is used to heat the 2DES, whereas the other, operating at low power, can probe the time scale on which the electrons relax their energy. By changing the time delay

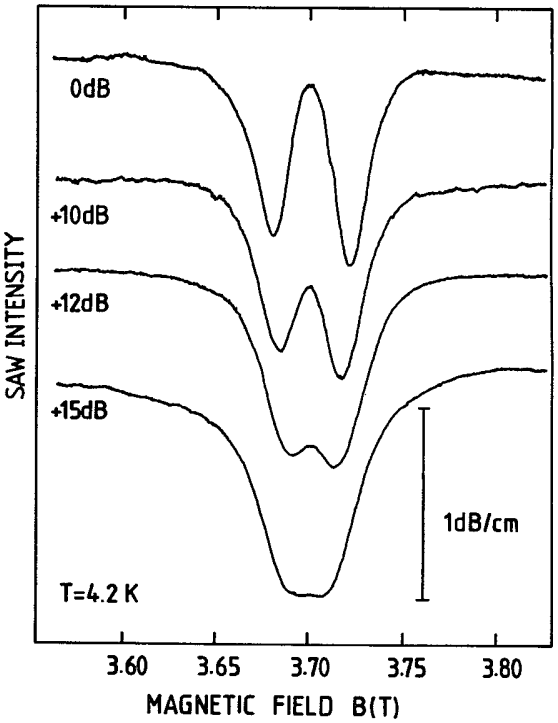

FIG. 9. Quantum oscillation in the transmitted SAW intensity for filling factor $\nu\simeq 4$ as function of the magnetic field B. The sample is identical to the one of Fig. 8. Parameter is the relative intensity of the high-frequency signal applied to the emitting transducer. With increasing power the splitting of the oscillation disappears and both minima merge on the B scale. This is interpreted in terms of an increased electron temperature as described in the text (from Ref. 11).

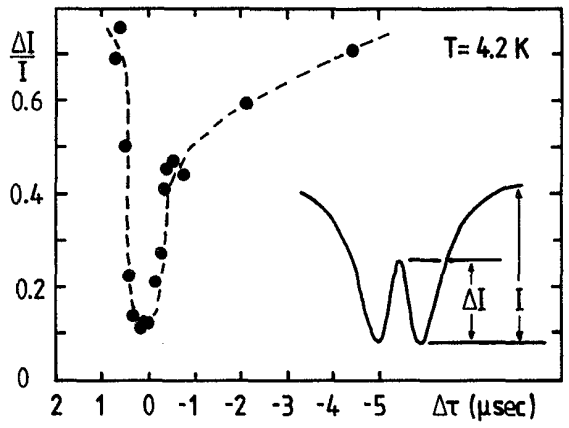

FIG. 10. Amount of splitting $\Delta I/I$ of a $\nu=4$ quantum oscillation in the transmitted SAW intensity as obtained in a time-resolved "heat and probe" experiment. $\Delta I/I$ is given as a function of the time delay $\Delta\tau$ between the heating and the probing SAW pulse. The wavelength of the high-power heating pulse is $\lambda_p=10$ μm, that of the low-power probing pulse is $\lambda_r=16$ μm. The splitting only disappears if both pulses completely overlap.

$\Delta\tau$ between the excitation of the pulses we can vary their actual spatial separation on the sample. A delay $\Delta\tau=0$ corresponds to the complete overlap of the two SAW packets. The result of such an experiment is shown in Fig. 10. Here, the amount of splitting $\Delta I/I$ of an oscillation of the probing pulse amplitude is plotted against the time delay $\Delta\tau$ between the heating and the probing pulse. A substantial decrease of $\Delta I/I$ is only observed for $\Delta\tau\approx 0$, i.e., if both SAW packets completely overlap. We thus conclude that within the time resolution of our experiments (approximately 50 ns), mainly given by the finite length of the SAW packets, the heating effect is instantaneous. We can therefore rule out lattice heating as cause for the activation, since such an effect has a time constant in the range of msec.

C. Line shape of the quantum oscillations in the SAW intensity

Here, we want to discuss in detail the line shape of quantum oscillations in the transmitted SAW intensity $I(B)$ that are split in high magnetic fields, i.e., at low filling factors ν. the main difference between the model presented in Sec. II and the experimentally observed line shape is the fact that for a given minimum in $\sigma_{xx}(B)$ the two observed minima in the SAW intensity have different depths. This observation is consistently made on most of the samples investigated. Equation (8) predicts that the maximum attenuation of the SAW per unit length is given by $\Gamma_{max}=kK^2_{eff}/4$. Hence, for a given interaction length L the minimum value of intensity transmitted through the heterojunction region is $L_{min}=I_0\exp(-\Gamma_{max}L)$. This value should be the same for all double minima in $I(B)$. As it has been shown,[18] this is only true if one assumes the conductivity $\sigma_{xx}(B)$ to be perfectly homogeneous across the whole heterojunction area $F=WL$. Here W is the width of the Hall bar that is covered by the SAW. The detected SAW signal $I(B)$ is proportional to the width W, since a transducer integrates over its aperture. In the small signal approximation which is valid here with $\Gamma L\ll 1$, we can write $I(B)\simeq I_0(1-\Gamma l)$ where l now is an effective interaction length given by $l=F/W$. We now assume the carrier distribution on the heterojunction area to be inhomogeneous. For simplicity, we consider several independent homogeneous domains of area F_i, each of which has a somewhat different conductivity $\sigma^i_{xx}(B)$ and thus a slightly different $\Gamma_i(B)$. The total transmitted SAW intensity then will be

$$I_{tot}\simeq I_0(1-\sum_i \Gamma_i l_i)\,. \tag{10}$$

Here, $l_i=F_i/W$ and $\sum_i F_i=F$. Different carrier densities N_{si} in the different domains cause different attenuations $\Gamma_i(B)$. For a given magnetic field these correspond to slightly different filling factors $\nu_i=N_{si}h/eB$.

A simulation of the influence of such small inhomogeneities on the transmitted SAW intensity is depicted in Fig. 11. Here we only assume two domains of different density and model each minimum in $\sigma^i_{xx}(B)$ by a parabola. This model results in an asymmetry in the split oscillation of the SAW intensity $I(B)$. To confirm our assumption of the role of inhomogeneities on the line shape of split quantum oscillations in $I(B)$, we have studied a sample in which we have intentionally created two domains of different carrier densities. For that purpose a small area ($\simeq 15\%$) of the sample is illuminated by a focused light emitting diode (LED) for short periods of time. Due to the persistent photoeffect[29,30] we thus can successively increase the carrier density N_s in the illuminated domain. The result of such an experiment is shown in Fig. 12, where the development of a split oscillation in $I(B)$ under illumination is depicted.

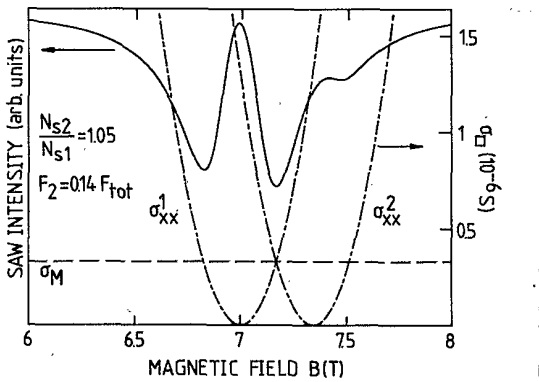

FIG. 11. Simulation of the influence of a small spatial inhomogeneity in the carrier density on the line shape of a split quantum oscillation in the SAW intensity (solid line). For simplicity, two discrete carrier density domains are assumed. The smaller one has conductivity σ^2_{xx} and covers 14% of the active sample area. It has a density N_{s2} that is only 5% larger than the one of the dominant domain (N_{s1}, σ^1_{xx}). The B dependence of σ^1_{xx} and σ^2_{xx} is included by the dashed line.

The increase in carrier density on a small part of the sample changes the line shape of the oscillation in the SAW intensity and finally leads to a shoulder on the high field side. This shoulder indicates the second, higher density area. It should be noted that the influence of such small inhomogeneities is difficult to extract from measurements of the magnetoresistance components ρ_{xx} and ρ_{xy}, respectively. Though one can observe small changes in ρ_{xx} with illumination, the measured changes depend crucially on the geometry of the potential probes used. The Hall plateaus in the measured Hall resistance ρ_{xy} are broadened by inhomogeneity of the carrier density which can be seen in Fig. 13. Here the quantum oscillations in the SAW intensity $I(B)$ and the corresponding plateaus in ρ_{xy} are shown as a function of the magnetic field. The traces in Fig. 13(b) correspond to the situation where two different carrier densities are present on the sample, leading to broadened Hall plateaus in ρ_{xy}. To study such spatial inhomogeneities, the surface wave technique proves advantageous. Since a SAW integrates over the whole sample area, it can directly yield information about the spatial uniformity of the 2DES under QHE conditions. Such information is difficult to deduce from studies of the magnetoresistance component ρ_{xx}, since there the averaging process is not yet known.

In some cases it is necessary to include a parallel conductance in the doped AlGaAs layer as another important parameter to describe the observed line shapes.[31,32] Since a SAW experiment is very sensitive in the range of small sheet conductivities, it also is a sensitive probe for such bypass conductivities in $GaAs/Al_xGa_{1-x}As$ heterostructure samples. A conducting bypass of areal conductivity $\sigma_{by} \lesssim \sigma_M$ will partially screen the SAW electric field at the plane of the 2DES and thus modify the intensity modulation $I(B)$ occurring in a split oscillation. A bypass with $\sigma_{by} > \sigma_M$ will prohibit splitting of the $I(B)$ oscillations even when $\sigma_{xx}(B)$ drops below σ_M. In heterojunctions with a large bypass conductivity $\sigma_{by} \gg \sigma_M$ the SAW electric field may be so strongly screened that quantum oscillations in $I(B)$ are hardly discernible even when σ_{xx} has deep minima.

If we neglect the small spacing between the bypass and

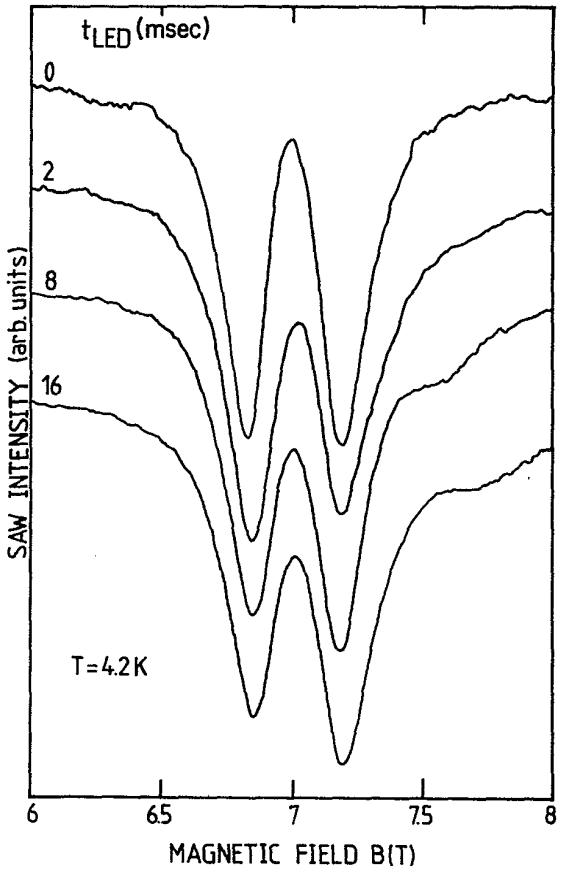

FIG. 12. Influence of an intentionally induced inhomogeneity on the line shape of a split quantum oscillation in the SAW intensity. A domain of higher electron density is created via the persistent photoeffect by local illumination of approximately 15% of the total sample area using a focused LED. The parameter t_{LED} is the accumulated illumination time which is a measure of the increased density in the illuminated domain (from Ref. 18).

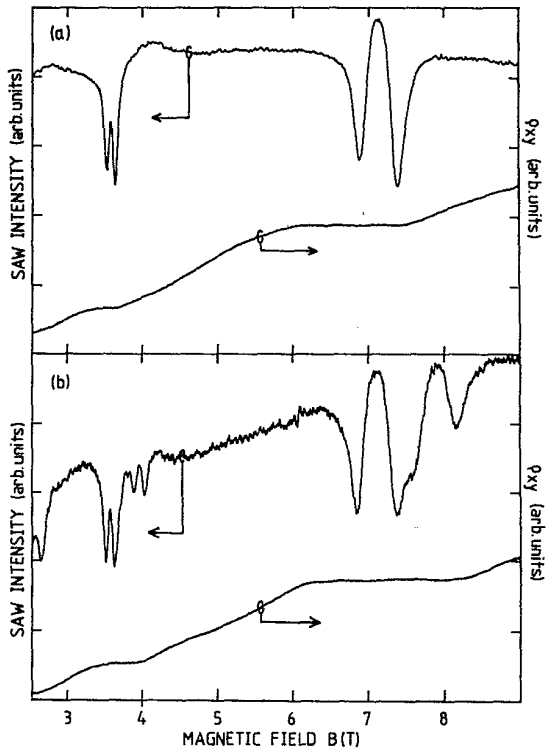

FIG. 13. Quantum oscillations in the transmitted SAW intensity $I(B)$ and simultaneously recorded Hall resistance $\rho_{xy}(B)$ at $T=4.2$ K. (a) represents a rather homogeneous sample with an electron density $N_s=3.4\times10^{11}$ cm^{-2}, such that $\nu=2$ is reached at $B=7.1$ T. In (b) two distinct carrier densities are present as indicated by two sets of split quantum oscillations in $I(B)$. This inhomogeneity significantly broadens the Hall plateaus.

the 2DES, we can include bypass influences by replacing in Eq. (8) $\sigma_\square$ by $\sigma_\square = \sigma_{xx} + \sigma_{by}$ and assume σ_{by} to be independent of magnetic field for the field range of a single quantum oscillation in $\sigma_{xx}(B)$. A homogeneous bypass on a homogeneous sample thus will act so as to effectively increase $\sigma_\square$ and to decrease splitting as well as the center maximum of a given $I(B)$ oscillation. It is possible to decrease σ_{by} without significantly changing σ_{xx} in gated heterostructures by applying a small gate bias. This is demonstrated in Fig. 14. Here, the heterostructure sample is part of a sandwich structure, in which the SAW propagates on a thinned $LiNbO_3$ delay line as sketched in Fig. 7. The gate voltage is applied between the metallized backside of this insulator and the 2DES. With increasing gate voltage one can see the occurrence of the splitting of the quantum oscillation, whereas the position on the B scale remains nearly unchanged. This indicates that the application of a small bias first depletes the bypass channel and then the 2DES.

By introducing a bypass conductivity in our calculation, we are able to model even very asymmetric line shapes, which is demonstrated in Fig. 15. Here we compare a measured quantum oscillation in the SAW intensity with a modeled line shape. For simplicity we have only used two domains of different carrier densities N_{si} and bypass conductivities. Shown is a quantum oscillation at $\nu=6$, with $\sigma_{xx}(B)$ modeled by a parabola.

By use of the SAW technique we could also show that domains of slightly different carrier densities can be generated in a heterostructure sample by the application of drift field pulses between the source and drain contacts. Results of such an experiment are depicted in Fig. 16. Here, the measured SAW intensity around an integer filling factor as a function of the magnetic field is shown. Drift pulses of height E_p are applied between source and drain for short intervals (~ 5 μsec) at low repetition rate (10 kHz). During this time a low-power SAW packet is excited and detected on the same sample. Here, the SAW is only used to probe the effect of the drift pulse on the 2DES. In Fig. 16(a) the parameter is the height of the applied electric field pulse. With increasing pulse height one clearly observes the generation of a well-defined, higher density domain on the sample. This domain grows in area, as indicated by an increase in the absorption depth for the high field quantum oscillation in $I(B)$. The growth of this domain occurs at the expense of the remaining sample area occupied by the original, lower density. After switching off the electrical drift pulse, this electric-field-induced inhomogeneity remains persistent, comparable to the effect of illuminating the sample by band-gap radiation. In Fig. 16(b) we demonstrate that not only the height of the electric drift pulse is important for the induced inhomogeneity but also the number of

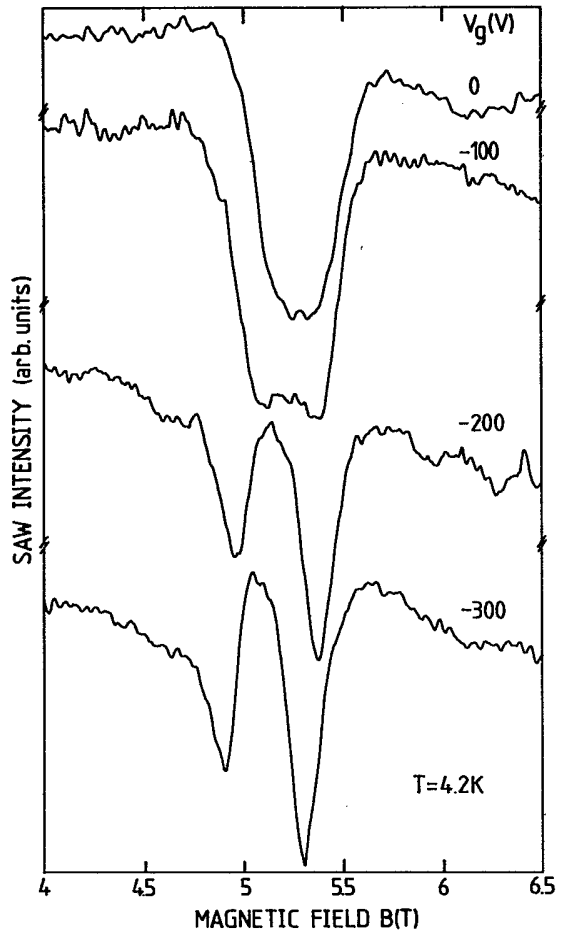

FIG. 14. Quantum oscillation of the transmitted SAW intensity around filling factor $\nu=2$ as measured on a sandwich structure consisting of a $LiNbO_3$ SAW delay line and a heterostructure sample. A negative gate voltage V_g is applied between the metallized backside of the delay line and the 2DES. As explained in the text a parasitic bypass conductivity $\sigma_{by} > \sigma_M$ in the doped AlGaAs layer suppresses splitting in the $I(B)$ oscillation at $V_g=0$ V. With increasing gate bias the bypass is depleted and splitting appears.

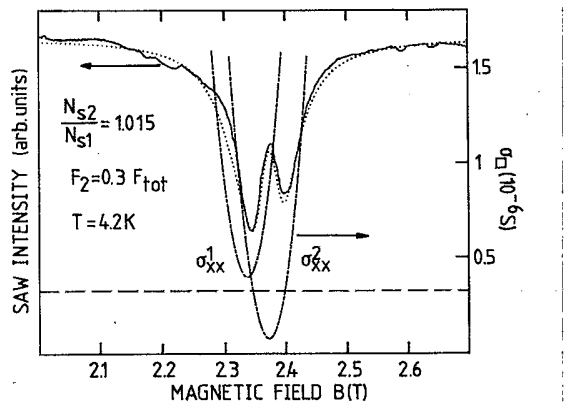

FIG. 15. Extended comparison of a measured split quantum oscillation (solid line) at filling factor $\nu=6$ in the SAW intensity and a simulation (dotted line) based on two domains of different density N_{si}, area F_i, channel conductivity σ^i_{xx}, and bypass conductivity σ^i_{by} ($i=1,2$) as indicated.

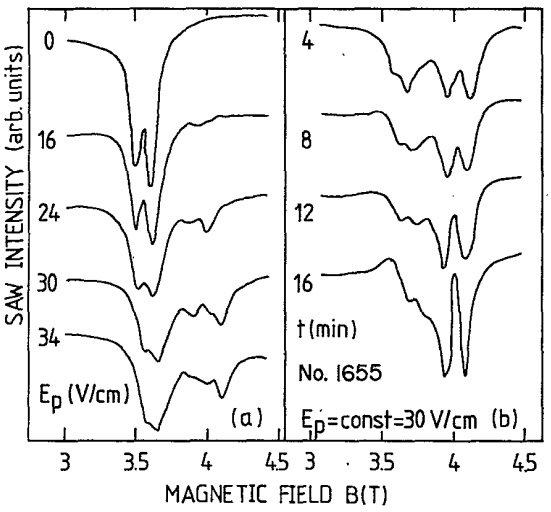

FIG. 16. Development of the $\nu=4$ quantum oscillation in the transmitted SAW intensity with application of short (5 μsec) source-drain drift pulses of strength E_p at a repetition rate of 10 kHz at a temperature of $T=4.2$ K. In (a) with increasing pulse amplitude a second higher density domain appears and increases. In (b) the accumulative effect of pulses of fixed heights E_p is studied. Here t is the total time for which pulses are applied (from Ref. 12).

pulses. Continuing the experiment with a constant amplitude of the drift pulses generating a field of $E_p=30$ V/cm, a further increase of the area occupied by the higher density domain is observed.

Similar results are obtained by replacing the electrical drift pulse by a high-power SAW pulse. Here too, a persistent inhomogeneity in the carrier density of the sample can be generated. Experimentally we find that in this case the strength of the magnetic field is important for generating inhomogeneities in the carrier density. This phenomenon we assume to be caused by the SAW electric field which is screened in the absence of magnetic fields and only becomes strong at magnetic fields corresponding to integer filling factors. At present, such electric-field-induced persistent inhomogeneities are not well understood. In particular, the electric fields that can generate such inhomogeneities are surprisingly low and seem to depend on the design of the heterojunctions. Further studies are needed to identify the origin of these phenomena.

In our opinion, SAW techniques are particularly useful to study the influence of small spatial inhomogeneities of a 2DES. Here we want to mention the relation between inhomogeneities and the apparent density of states between Landau levels.[33] The magnetic field dependence of many quantities that depend on the density of states such as capacitance or specific heat have been successfully modeled by the assumption of a finite density of states between Landau levels. There have also been suggestions to explain the integer quantum Hall effect only on bases of small spatial inhomogeneities in the carrier density.[34] Here, SAW techniques may provide a test for this inhomogeneity model of the quantum Hall effect.

D. Frequency dependence

The frequency dependence of the interaction between a SAW and a 2DES has been studied on various samples with transducers of different periodicities.[12] This is necessary, since for an interdigital transducer of a given period p only a narrow frequency band is accessible. Therefore we either have to change the transducer geometry or to operate the transducer on higher harmonics. We have prepared different transducer structures on the same sample such that we can excite several SAW frequencies on the same heterostructure. The results of such experiments are summarized in Fig. 17. Here we plot the maximum attenuation Γ_{max} as obtained from measurements of the minimum transmitted SAW intensity versus the SAW frequency. The relaxation model as expressed by Eq. (8) predicts a linear increase of this maximum attenuation with frequency or wave number of the SAW and is given by $\Gamma_{max}=kK^2_{eff}/4$. In Fig. 17 the solid line depicts the expected frequency dependence of Γ_{max}, using a sound velocity of $v_0=2959$ m/sec and an effective electromechanical coupling coefficient $K^2_{eff}=6.4\times10^{-4}$. Both values agree very well with those found in literature.[19] For frequencies up to 300 MHz or, equivalently, for wavelengths down to approximately 10 μm no significant deviation is observed from the linear dependence within experimental error. For higher frequencies we consistently observe deviations corresponding to a decrease in the slope $d\Gamma_{max}/d\omega$. Within the relaxation time model we cannot describe the deviation and a more sophisticated theory would be needed. Such a theory should include nonlocal corrections of the interaction between a SAW and a 2DES. For high frequencies the SAW wavelength may become comparable to intrinsic lengths l_{int} in the 2DES and thus $kl_{int}\approx1$ which would cause nonlocal effects to be reflected in the SAW attenuation. These intrinsic lengths may be related to localization in the quantum Hall regime or to diffusion effects that have been neglected up to now.

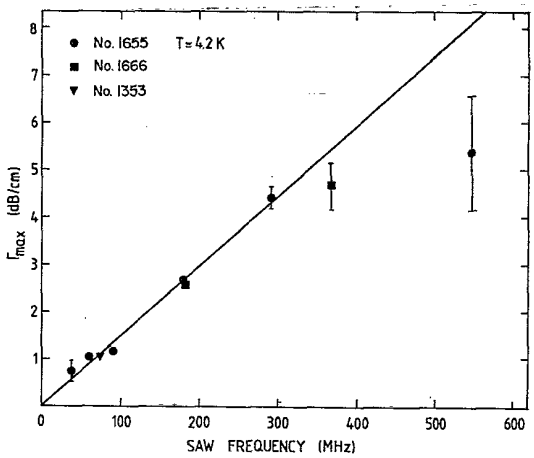

FIG. 17. Frequency dependence of the maximum attenuation Γ_{max} of a SAW by a 2DES. Different samples are labeled by the wafer number.

E. Gated heterostructures

We recently succeeded in observing the interaction of surface acoustic waves and a 2DES in gated heterostructures. Here, we are able to control the carrier density and hence the conductivity of the 2DES by use of a front gate electrode. Between the surface of the heterojunction sample and the gate electrode we deposit a thin insulating photoresist layer to increase the distance between the metal electrode and the 2DES to avoid shortening of the SAW electric field. The thickness of this layer is of the order of some hundred nm, still much smaller than typical SAW wavelengths. The SAW on these gated samples thus propagates on the interface between the photoresist layer and the heterostructure sample. The distribution of the piezoelectric potential here is more complicated than depicted in Fig. 1, since there is no piezoelectricity in the insulating photoresist layer.

First experimental results concerning the interaction between a SAW and a 2DES in gated heterostructures are shown in Fig. 18 for two different samples. In Fig. 18(a) the transmitted SAW intensity is plotted versus the magnetic field for different gate voltages V_g. The SAW wavelength for this sample is $\lambda=16\ \mu$m and the thickness of the photoresist layer is $d=460$ nm. Hence the total distance of the gate electrode from the plane of the 2DES is about 4% of the SAW wavelength. The threshold gate voltage at which complete depletion of the 2D channel occurs is around $V_{th}\simeq -8$ V. By varying the gate voltage between $V_g=0$ V and $V_g=-4$ V the carrier density of the sample can be reduced from $N_s(0\ \text{V})\simeq 3.6\times10^{11}$ cm^{-2} down to $N_s(-4\ \text{V})\simeq 1.8\times10^{11}$ cm^{-2}. This is clearly seen by a shift of the corresponding quantum oscillations in $I(B)$ towards lower magnetic fields.

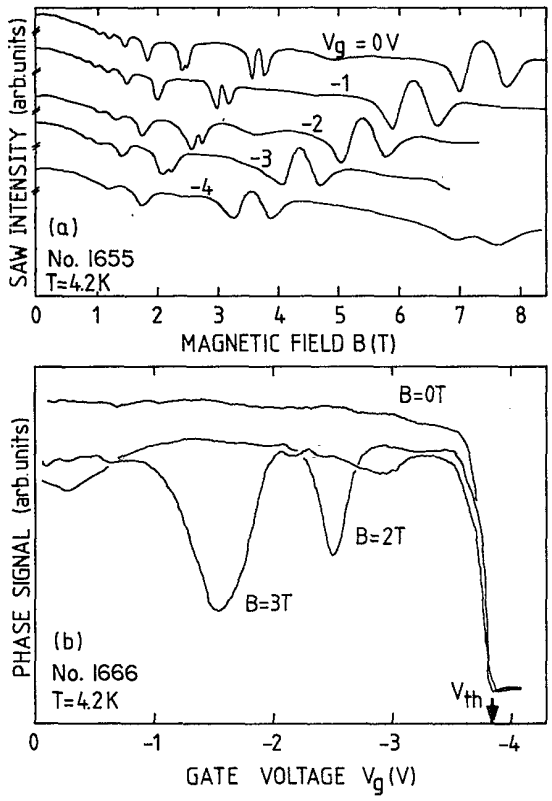

FIG. 18. First experimental results for the interaction of a SAW with a 2DES on gated heterojunctions. For the sample in (a) we display the magnetic field dependence of the SAW intensity at different gate voltages V_g. For the sample in (b) we show the gate voltage dependence of the SAW phase signal at two magnetic fields B and $B=0$ T. V_{th} indicates the inversion threshold.

For a different sample, we show in Fig. 18(b) the detected phase signal of the SAW as a function of the gate voltage for different magnetic fields. The insulating photoresist layer on this sample has a thickness of $d=300$ nm and the SAW wavelength is $\lambda=8\ \mu$m. The smaller insulator thickness leads to a smaller threshold gate voltage, in this case $V_{th}\simeq -3.8$ V as indicated by an arrow. The pronounced quantum oscillations in the $B=2$ T and $B=3$ T traces correspond to the change in sound velocity caused by the minimum in σ_{xx} around the filling factor $\nu=2$. The sharp step around $V_g\simeq V_{th}$ indicates the piezoelectric stiffening in the conductivity range $\sigma_{xx}\lesssim\sigma_M$ near inversion threshold. There the interaction between the SAW and a 2DES may be investigated even in the absence of magnetic fields, as σ_{xx} always drops below σ_M for V_g approaching V_{th}.

V. CONCLUSION AND PERSPECTIVES

We have studied the interaction between surface acoustic waves and quasi-two-dimensional electron systems in GaAs/$Al_xGa_{1-x}As$ heterostructures. At low temperatures and in high magnetic fields we observe quantum oscillations in the propagation parameters, namely the intensity and the sound velocity of the SAW. These oscillations reflect the Shubnikov–de Haas oscillations of the magnetoconductivity of the 2DES. Moreover, the interaction between the SAW and a 2DES becomes strongest in magnetic field regions where the magnetoconductivity $\sigma_{xx}(B)$ drops to very low values, i.e., in the regime of the quantum Hall effect. We have shown that even there the interaction can be described quasiclassically by a simple relaxation-type model in which the 2DES influences the SAW solely via its sheet conductivity.

The integrative character of SAW experiments makes them very sensitive to changes in the spatial distribution of the sheet conductivity or the carrier density on the sample area. This we use to semiquantitatively describe the line shape of the observed quantum oscillations in the SAW intensity by assuming very small inhomogeneities in the areal carrier density. Such small inhomogeneities and their influence on, e.g., the quantum Hall effect are in general not visible in standard dc magnetoresistance experiments. We also show that spatial inhomogeneities in the carrier density can be generated if electrical drift pulses are applied to the 2DES via source-drain contacts. Here, SAW experiments again prove a sensitive tool for studies of spatial inhomogeneity.

At high SAW intensities the quantum oscillations of the transmitted SAW intensity show a characteristic dependence on the amplitude o the SAW. We interpret

this behavior as an increase of the electron temperature in the electric field of the surface wave. Experimentally we show that this "phonoconductive" response is instantaneous within the time resolution of our experiment.

Further, we have studied the frequency dependence of the interaction by using different SAW wavelengths. Up to frequencies of 300 MHz or, equivalently, down to wavelengths of 10 μm no deviations from the behavior predicted by the simple classical model are observed. For higher frequencies or shorter wavelengths we consistently observe a decrease in the maximum attenuation which will be the subject of further investigations.

We have demonstrated that interaction of a SAW with a 2DES also can be observed in a sandwich structure where the SAW is excited and detected on a separate piezoelectric medium. Here the 2DES interacts with the electric field of the SAW by means of proximity coupling. This very simple, contactless, and nondestructive technique is a useful tool for the characterization of heterostructure samples without the need for special sample preparation.

Finally, we have presented initial experimental results on the interaction of surface acoustic waves with a 2DES in gated heterojunction samples. Here, we can control the carrier density and hence the conductivity of the 2DES by use of a front gate electrode. This way, a new field of investigations is opened. We now can study the interaction between a SAW and a 2DES on samples with very low carrier densities. In high magnetic fields and at low temperatures we thus should be able to enter the regime of the fractional quantum Hall effect and the transition of the 2DES to the Fermi liquid state. Also, experiments on samples with laterally microstructured gate electrodes become accessible. Thus we may hope to study the interaction between SAW's and quasi-one-dimensional electron systems (1DES).[35] Another important aspect of gated heterostructure samples is the possibility of acoustic charge transport in the potential wells of the SAW. This should be observable if the 2D channel is depleted to just above threshold, i.e., at very low carrier densities. Beside the scientific interest this heterojunction acoustic charge transport can play an important role in rf signal processing devices.[36] Studies of the interaction of a SAW and a 2DES near conductance threshold make experiments possible even at zero magnetic field. By application of a gate bias we can cover the range of conductivity where the interaction becomes strongest, i.e., $\sigma \approx \sigma_M$. At the same time the mobility of the carriers in the system remains nearly unchanged. This gives rise to the question of whether acoustic amplification[35] can be observed in these systems.

ACKNOWLEDGMENTS

We would like to thank A. V. Chaplik for stimulating and fruitful discussions concerning theoretical aspects of this work. The $LiNbO_3$ substrates have been kindly provided by Ch. Grabmeier (Siemens Forschungslabor, München). Financial support of the Deutsche Forschungsgemeinschaft (Bonn, Germany) is gratefully acknowledged.

*Present address: University of California, Santa Barbara, Santa Barbara, California 93106.

[1]For a comprehensive review see, e.g., T. Ando, A. B. Fowler, and F. Stern, Rev. Mod. Phys. **54**, 437 (1982).

[2]For a recent review on spectroscopy in the ir regime see, e.g., U. Merkt, in *Festkörperprobleme (Advances in Solid State Physics)*, edited by P. Grosse (Vieweg, Braunschweig, 1987), Vol. 27, pp. 109–136.

[3]For a recent summary on Raman spectroscopy see, e.g., G. Abstreiter, M. Cardona, and A. Pinczuk, in *Light Scattering in Solids IV*, edited by M. Cardona and G. Güntherodt (Springer, Berlin, 1984), pp. 5–150.

[4]For a recent review see, e.g., D. Weiss, K. v. Klitzing, and V. Mosser, in *Two Dimensional Systems: Physics and New Devices*, edited by G. Bauer, F. Kuchar, and H. Heinrich (Springer, Berlin, 1986), p. 204.

[5]For a recent review see, e.g., R. Lassnig and E. Gornik, in *Two Dimensional Systems: Physics and New Devices*, edited by G. Bauer, F. Kuchar, and H. Heinrich (Springer, Berlin, 1986), p. 218.

[6]K. v. Klitzing, G. Dorda, and M. Pepper, Phys. Rev. Lett. **45**, 494 (1980).

[7]D. C. Tsui, H. L. Störmer, and A. C. Gossard, Phys. Rev. Lett. **48**, 1559 (1982).

[8]For a comprehensive review see, e.g., L. J. Challis, G. A. Toombs, and F. W. Sheard, in *The Physics of Phonons*, Vol. 285 of *Springer Lecture Notes in Physics*, edited by T. Paskiewicz (Springer, Berlin, 1987), p. 348.

[9]J. C. Hensel, R. C. Dynes, and D. C. Tsui, Phys. Rev. B **28**, 1124 (1983).

[10]M. Rothenfusser, L. Köster, and W. Dietsche, Phys. Rev. B **34**, 5518 (1986).

[11]A. Wixforth, J. P. Kotthaus, and G. Weimann, Phys. Rev. Lett. **56**, 2104 (1986).

[12]A. Wixforth and J. P. Kotthaus, in *The Application of High Magnetic Fields in Semiconductor Physics*, edited by G. Landwehr (Springer, Berlin, in press).

[13]F. Kuchar, R. Meisels, G. Weinmann, and W. Schlapp, Phys. Rev. B **33**, 2965 (1986).

[14]P. Das, M. E. Montamedi, and R. T. Webster, Appl. Phys. Lett. **27**, 120 (1975).

[15]For a review see, e.g., *Acoustic Surface Waves*, Vol. 24 of *Topics in Applied Physics*, edited by A. A. Oliner (Springer, Berlin, 1978).

[16]A. Schenstroem, Y. J. Quian, M. F. Xu, H. P. Baum, H. Levy, and B. K. Sarma, Solid State Commun. **65**, 739 (1988).

[17]A. Wixforth, J. Scriba, M. Wassermeier, J. P. Kotthaus, G. Weimann, and W. Schlapp, Appl. Phys. **64**, 2213 (1988).

[18]A. Wixforth, J. Scriba, M. Wassermeier, J. P. Kotthaus, G. Weimann, and W. Schlapp, in *Proceedings of the 19th International Conference on the Physics of Semiconductors, Warsaw, 1988*, edited by W. Zawadski (Institute of Physics, Polish Academy of Sciences, Warsaw, 1988).

[19]R. T. Webster and P. H. Carr, in *Rayleigh Waves, Theory and Applications*, Vol. 2 of *Springer Series on Wave Phenomena*, edited by E. A. Ash and E. G. S. Paige (Springer, Berlin, 1985), pp. 122–130.

[20]A. R. Hutson and D. L. White, J. Appl. Phys. **33**, 40 (1969).

[21]K. A. Ingebrigsten, J. Appl. Phys. **41**, 454 (1972).
[22]R. Adler, IEEE Trans. Sonics Ultrason. **SU-18**, 115 (1971).
[23]P. Bierbaum, Appl. Phys. Lett. **21**, 595 (1972).
[24]A. V. Chaplik, Pis'ma Zh. Tekh. Fiz. **10**, 1385 (1984) [Sov. Tech. Phys. Lett. **10**, 584 (1984)].
[25]B. K. Ridley, Semicond. Sci. Technol. **3**, 542 (1988).
[26]J. H. McFee, in *Physical Acoustics,* edited by W. Mason (Academic, New York, 1966), Vol. 4A, pp. 1–47.
[27]G. Weimann, in *Festkörperprobleme (Advances in Solid State Physics),* edited by P. Grosse (Vieweg, Braunschweig, 1986), p. 231.
[28]R. M. White and T. W. Woltmer, Appl. Phys. Lett. **7**, 314 (1965).
[29]R. J. Nicholas, M. A. Brummell, J. C. Portal, G. Gregoris, S. Hersee, and J. P. Duchemin, Appl. Phys. Lett. **44**, 629 (1984).
[30]T. N. Theis and S. L. Wright, Appl. Phys. Lett. **48**, 1374 (1986).
[31]E. F. Schubert, K. Ploog, H. Dämbkes, and K. Heime, Appl. Phys. A **33**, 63 (1984).
[32]M. J. Kane, N. Apsley, D. A. Anderson, L. L. Taylor, and T. Kerr, Phys. C **18**, 5629 (1985).
[33]V. Gudmundsson and R. R. Gerhardts, Phys. Rev. B **35**, 8005 (1987).
[34]R. Woltjer, R. Eppenga, J. Mooren, C. E. Timmering, and J. P. Andre, Europhys. Lett. **2**, 149 (1986).
[35]W. Hansen, M. Horst, U. Merkt, Ch. Sikorski, J. P. Kotthaus, and K. Ploog, Phys. Rev. Lett. **58**, 2586 (1987).
[36]M. J. Hoskins, H. Morkoç, and B. J. Hunsinger, Appl. Phys. Lett. **41**, 332 (1982).
[37]A. R. Hutson, J. H. McFee, and D. L. White, Phys. Rev. Lett. **7**, 237 (1961).